Evaluation of the common EOF approach in linear Empirical Downscaling of Future ECHAM4/OPYC3 GSDIO Climate Scenarios.

R.E. Benestad

DNMI, November 19, 1999

Contents

1 Introduction

Benestad (1999e) used global climate change scenarios from coupled general circulation models (GCMs) and empirical downscaling models in an attempt to predict changes to the local climate. Although the GCMs gave a good reproduction of the large scale geographical climate patterns, the matching of observed and simulated spatial patterns introduced additional uncertainties and the possibility of additional errors. Here, we have evaluated a technique which aims to eliminate these additional error sources by using *common empirical orthogonal functions (common EOFs)* (*Barnett*, 1999). The method, which is also described in this report, will henceforth be referred to as the *common EOF method*.

It is crucial to know how well the common EOF methodology predicts local climate statistics before using it to make future climate scenarios. The primary purpose of this report is therefore to give an evaluation of the common EOF downscaling method. Sensitivity experiments described here with different options give different downscale scenarios for Norway, and therefore these should not be taken as our predictions for the future before an objective downscaling configuration has been identified. Extensive studies on downscaled future climate scenarios will be left for later.

2 Methods

2.1 Data

The scenarios examined here were taken from the to date's latest Max-Planck-Institute's coupled transient climate run with the coupled general circulation model (CGCM) ECHAM4/OPYC3, with transient boundary conditions with greenhouse gases , direct, and indirect aerosol forcing (*GSDIO*). The CGCM is described in *Machenhauer* et al. (1998), *Benestad* et al. (1999) and *Benestad* (1999e). The *GSDIO* data have been converted to the *netCDF* format (*Rew* et al., 1996) and are described in *Benestad* (1999b). The transient greenhouse gas only (*GHG*) integration analysed by *Benestad* (1999e), on the other hand, were from an earlier model run, and therefore some of the differences between the results obtained here and those of *Benestad* (1999e) may be due to both different methodology and different GCM data. Moreover, the main differences between the *GSDIO* and *GHG* run is that *GSDIO* accounts for the effect of the aerosols whereas *GHG* only takes into account the forcing from greenhouse gases.

The predictands used here were monthly mean temperatures taken from

the Norwegian Meteorological Institute's (DNMI) archives.

2.2 Common EOFs

The common EOF method is a useful technique for extracting common spatial climate patterns in two or more data sets. The principle of the common EOF method is that two or more data fields with data points on a common grid are combined (concatenated), and an EOF analysis (*Benestad*, 1999f) is applied to the results. The common EOFs are explained in more detail by (*Barnett*, 1999). Here we have only combined two fields of same physical parameter, one which is made up of observations and one which consists of GCM model results, as a common spatial structure is sought. Figure 1 shows the 4 leading common EOFs calculated using 49 January monthly SLP values (1950-1997) from NCEP reanalysis (*Benestad*, 1996) and MPI GSDIO (*Benestad*, 1999b) respectively. These results were obtained after having detrended the observations prior to the EOF analysis. The simulated data, were not de-trended.

The advantage with the common EOF method is that they are eigenvectors which are assured to span both the observed and model data space. For conventional EOFs, on the other hand, there is no guarantee that the observed EOFs span the data space of the model results.

The common EOF method involves the computation of the common EOFs, of which the principal components[1] (PCs) which correspond to the observations are used for calibration of the empirical model. As the model PCs correspond to the same common EOF spatial patterns as the observed PCs, the empirical model obtained with the observations can be applied directly to the model PCs. Figure 2 illustrates the process of training the empirical model and then using the model in conjunction with the model PCs to make predictions.

The magnitude of the simulated fields, x_m, were scaled in order to describe similar variance levels as the observations, x_o: $x'_m = (x_m - \overline{x_m}) \times std(x_m)/std(x_o)$. This preprocessing step ensures similar weight to the model and observed fields, and provides an ad hoc correction for model misrepresentation of the variance in the predictor fields. Both observed and simulated fields were taken to have zero mean values.

[1] Defined here as the normalised time evolution of the spatial patterns, or T-EOFs (*Benestad*, 1999f).

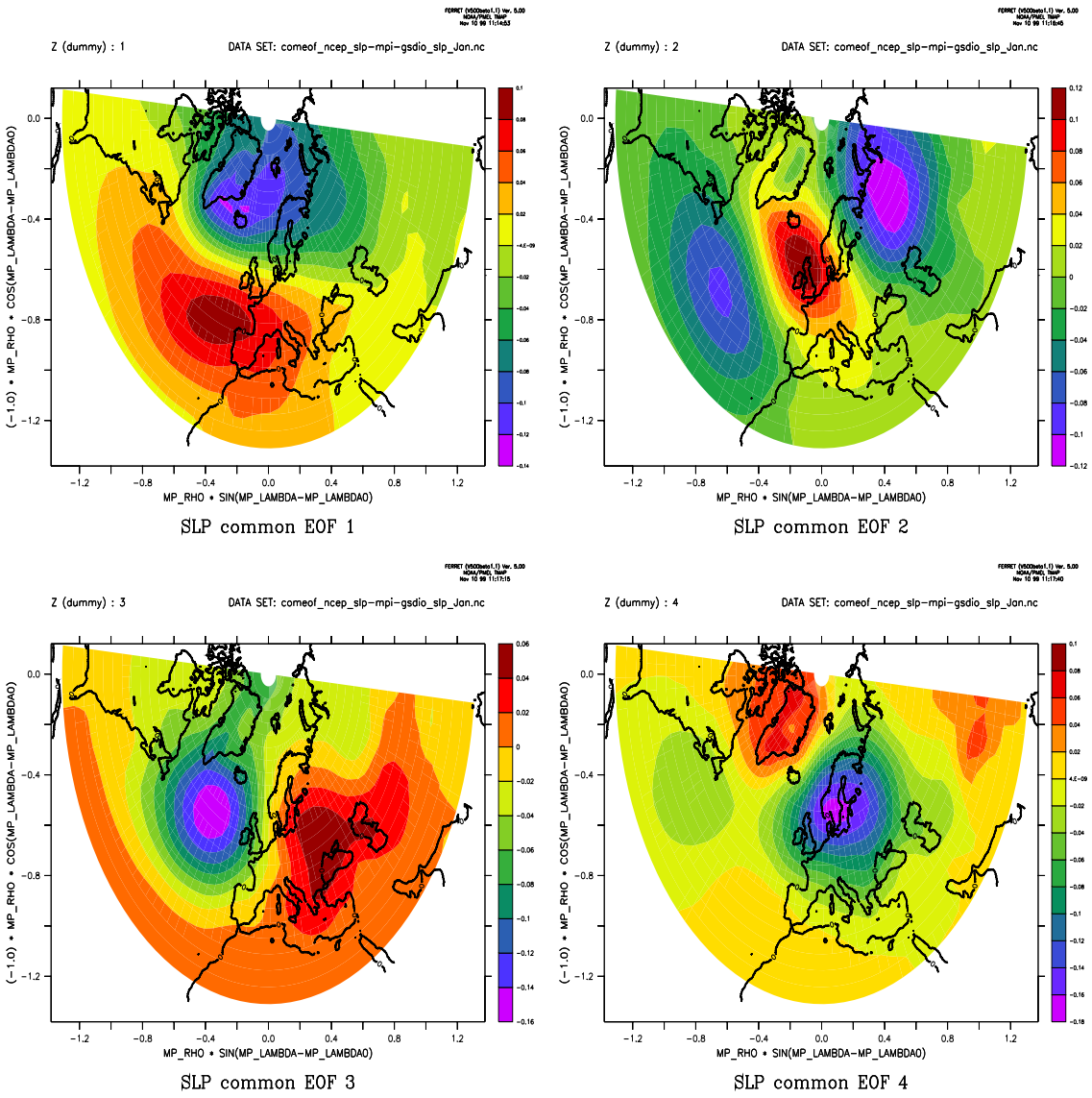

Figure 1: The 4 leading common EOFs based on MPI GSDIO and NCEP reanalysis SLP, each consisting of 49 years.

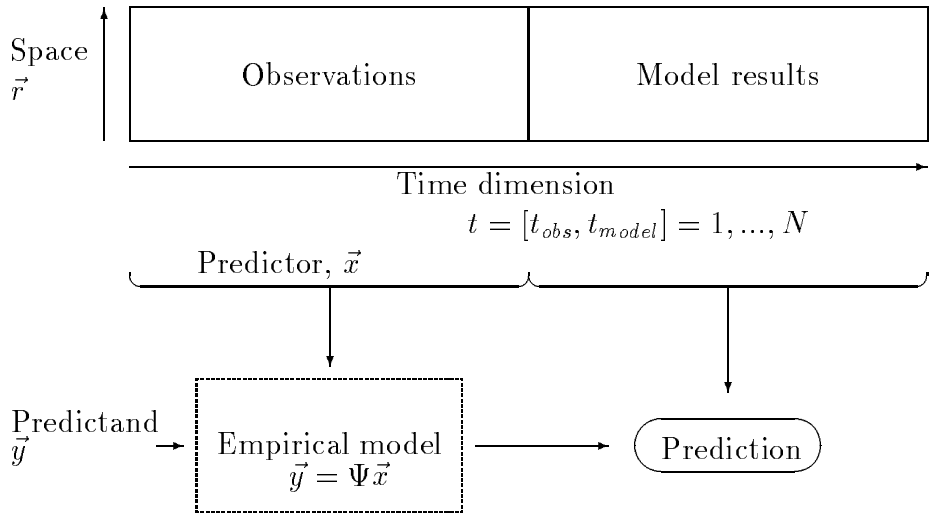

Figure 2: Schematic illustrating the common EOF method. Here, y denotes the predictands (station observations), x are the predictors (large scale circulation patterns) taken from the common EOF observed PCs ($t = [t_1, ..., t_N]$), and $\vec{r}$ represents a vector of M spatial points ($[r_1, ..., r_M]$).

2.3 Sensitivity experiments

There are several different ways to apply common EOFs to downscaling, and there are no clear optimal method a priori. The empirical model used in the standard method was based on a canonical correlation analysis (*Benestad*, 1998a, 1999e), but other linear method for making empirical models, such as singular value decomposition (SVD) (*Benestad*, 1998b) and multi-variate regression (MVR) (*Benestad*, 1999d), were also tried. Here, we will look at the results for downscaling experiments based on the NCEP January SLP fields, using a number of different approaches. We will refer to predictions using common EOFs where the model and observed fields describe similar standard deviations at each grid point, the length of the observational and model records are the same, and where the observations have been de-trended as the *standard procedure* (data file: comeof_ncep_slp-mpi-gsdio_slp_Jan.nc). In the standard downscaling exercise described here, only 47 points in time were used for model calibration (1950-1996), as the temperatures used here were not up to date.

One set of experiments, referred to as the *rescaling* experiments, involved a scaling of the predictions so that they had the same standard deviation as the cross-validated results from the calibration interval. Another set of experiments therefore looks at the importance of de-trending the data prior to the analysis. We also experiment with using different lengths in time for observed and model data records. Finally, the common EOF method is examined to see how robust it is with respect to different predictand combinations. *Benestad* (1999e) reported that the results for one given location may be sensitive to the choice of predictand group.

3 Results

Figure 3 shows the results of four of the experiments whereas tables 1 to 3 summarises the most important points of all experiments.

Figure 4 shows the temperature distributions and the residuals from the standard downscaling procedure. The temperature distributions hint at greater temperature range at Nesbyen (an inland station: upper top panel) than the other 3 locations with more coastal climate type. A time plot of the residuals from the model calibration (left, second from the bottom) shows a clear trend, suggesting that the empirical model did not capture the observed slow warming. These trends are in accordance with our expectations, as the linear trends in the predictor fields used for model calibration had been removed prior to model calibration. The fact that the trends in the

Table 1: Observed past (1890-1997) and predicted January temperature trends using SLP common EOFs.

Location	Obs. past warming (^oC/decade)	Projected warming (^oC/decade)	Correlation score	RMSE score (^oC)
Standard				
OSLO - BLINDERN	0.0920	0.2506	0.79	0.26
NESBYEN - SKOG.	0.1197	**0.4091**	0.72	0.44
FERDER FYR	0.1238	0.1822	0.84	0.22
OKSOEY FYR	0.0627	0.1761	0.86	0.19
Re-scaled				
OSLO - BLINDERN	0.0920	0.6003	0.79	0.26
NESBYEN - SKOG.	0.1197	**0.9804**	0.72	0.44
FERDER FYR	0.1238	0.4635	0.84	0.22
OKSOEY FYR	0.0627	0.4710	0.86	0.19
Different lengths				
OSLO - BLINDERN	0.0920	0.0867	0.79	0.26
NESBYEN - SKOG.	0.1197	0.1448	0.75	0.41
FERDER FYR	0.1238	0.1121	0.83	0.22
OKSOEY FYR	0.0627	0.0871	0.86	0.19
Obs. w trend				
OSLO - BLINDERN	0.0920	0.1603	0.82	0.25
NESBYEN - SKOG.	0.1197	0.3105	0.79	0.39
FERDER FYR	0.1238	0.1387	0.84	0.22
OKSOEY FYR	0.0627	0.1350	0.87	0.19
Stationgroup II				
OSLO - BLINDERN	0.0920	0.2368	0.80	0.26
NESBYEN - SKOG.	0.1197	0.3771	0.74	0.43
Stationgroup III				
OSLO - BLINDERN	0.0920	0.2085	0.79	0.27
FERDER FYR	0.1238	0.1439	0.84	0.22
OKSOEY FYR	0.0627	0.1483	0.86	0.19
Stationgroup IV				
OSLO - BLINDERN	0.0920	0.2229	0.79	0.27
FERDER FYR	0.1238	0.1625	0.84	0.22
Stationgroup V				
OSLO - BLINDERN	0.0920	0.2270	0.79	0.27
OKSOEY FYR	0.0627	0.1645	0.86	0.20

Table 2: Observed past (1890-1997) and predicted January temperature trends using SLP common EOFs.

Location	Obs. past warming (^oC/decade)	Projected warming (^oC/decade)	Correlation score	RMSE score (^oC)
NATL II 90W-40E, 40N-75N				
OSLO - BLINDERN	0.0920	0.0471	0.46	0.38
NESBYEN - SKOG.	0.1197	0.1290	0.31	0.61
NORDIC II 20W-40E, 50N-75N				
OSLO - BLINDERN	0.0920	**0.0705**	0.40	0.40
NESBYEN - SKOG.	0.1197	**0.1898**	0.30	0.61
SCAN II 0W-30E, 55N-75N				
OSLO - BLINDERN	0.0920	**0.3214**	0.48	0.38
NESBYEN - SKOG.	0.1197	**0.4580**	0.40	0.58
NATL V 90W-40E, 40N-75N				
OSLO - BLINDERN	0.0920	0.0562	0.48	0.38
OKSOEY FYR	0.0627	0.0199	0.46	0.34
NORDIC V 20W-40E, 50N-75N				
OSLO - BLINDERN	0.0920	**0.0703**	0.40	0.40
OKSOEY FYR	0.0627	**0.0609**	0.35	0.36
SCAN V 0W-30E, 55N-75N				
OSLO - BLINDERN	0.0920	**0.2753**	0.48	0.38
OKSOEY FYR	0.0627	0.1560	0.40	0.35
SVD II				
OSLO - BLINDERN	0.0920	0.1186	0.79	0.26
NESBYEN - SKOG.	0.1197	0.2537	0.74	0.43
NATL SVD II 90W-40E, 40N-75N				
OSLO - BLINDERN	0.0920	0.1379	0.44	0.39
NESBYEN - SKOG.	0.1197	0.2228	0.32	0.60
NORDIC SVD II 20W-40E, 50N-75N				
OSLO - BLINDERN	0.0920	0.0706	0.24	0.42
NESBYEN - SKOG.	0.1197	**0.2795**	0.27	0.61
SCAN SVD II 0W-30E, 55N-75N				
OSLO - BLINDERN	0.0920	**0.2278**	0.22	0.42
NESBYEN - SKOG.	0.1197	**0.2452**	0.12	0.63

Table 3: Observed past (1890-1997) and predicted January temperature trends using SLP common EOFs.

Location	Obs. past warming (^oC/decade)	Projected warming (^oC/decade)	Correlation score	RMSE score (^oC)
NATL SVD V 90W-40E, 40N-75N				
OSLO - BLINDERN	0.0920	**0.2293**	0.40	0.40
OKSOEY FYR	0.0627	**0.1403**	0.36	0.36
NORDIC SVD V 20W-40E, 50N-75N				
OSLO - BLINDERN	0.0920	**0.2614**	0.23	0.43
OKSOEY FYR	0.0627	**0.1938**	0.18	0.38
SCAN SVD V 0W-30E, 55N-75N				
OSLO - BLINDERN	0.0920	**0.2424**	0.22	0.42
OKSOEY FYR	0.0627	**0.1896**	0.26	0.37
MVR II				
OSLO - BLINDERN	0.0920	**0.2647**	0.81	0.26
NESBYEN - SKOG.	0.1197	**0.4317**	0.69	0.46
NATL MVR II 90W-40E, 40N-75N				
OSLO - BLINDERN	0.0920	**0.2162**	0.43	0.40
NESBYEN - SKOG.	0.1197	0.3002	0.36	0.60
NORDIC MVR II 20W-40E, 50N-75N				
OSLO - BLINDERN	0.0920	0.0688	0.41	0.40
NESBYEN - SKOG.	0.1197	**0.1839**	0.31	0.62
SCAN MVR II 0W-30E, 55N-75N				
OSLO - BLINDERN	0.0920	0.0563	0.48	0.38
NESBYEN - SKOG.	0.1197	0.1379	0.34	0.60
NATL MVR V 90W-40E, 40N-75N				
OSLO - BLINDERN	0.0920	0.0563	0.48	0.38
OKSOEY FYR	0.0627	0.0174	0.46	0.34
NORDIC MVR V 20W-40E, 50N-75N				
OSLO - BLINDERN	0.0920	**0.2753**	0.48	0.38
OKSOEY FYR	0.0627	0.1560	0.40	0.35
SCAN MVR V 0W-30E, 55N-75N				
OSLO - BLINDERN	0.0920	**0.2162**	0.43	0.40
OKSOEY FYR	0.0627	**0.1048**	0.36	0.36

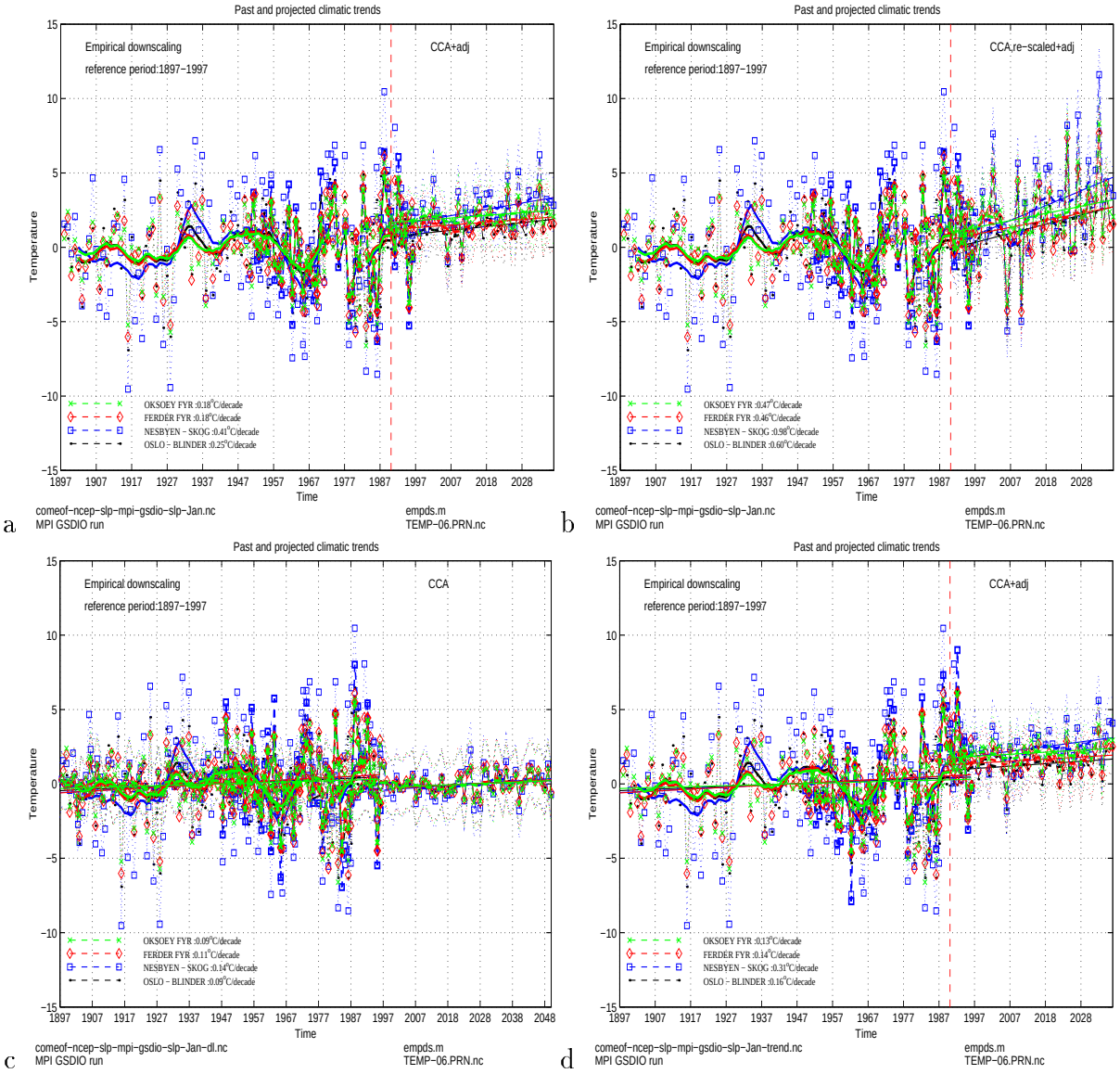

Figure 3: Various experimental downscaled results for selected stations in southern Norway, for standard procedure (a), results from standard procedure re-scaled to yield same standard deviation as cross-validation results (b), using common EOFs estimated with different time lengths for observations and model results (c), and using standard procedure, but without de-trending the observations (d).

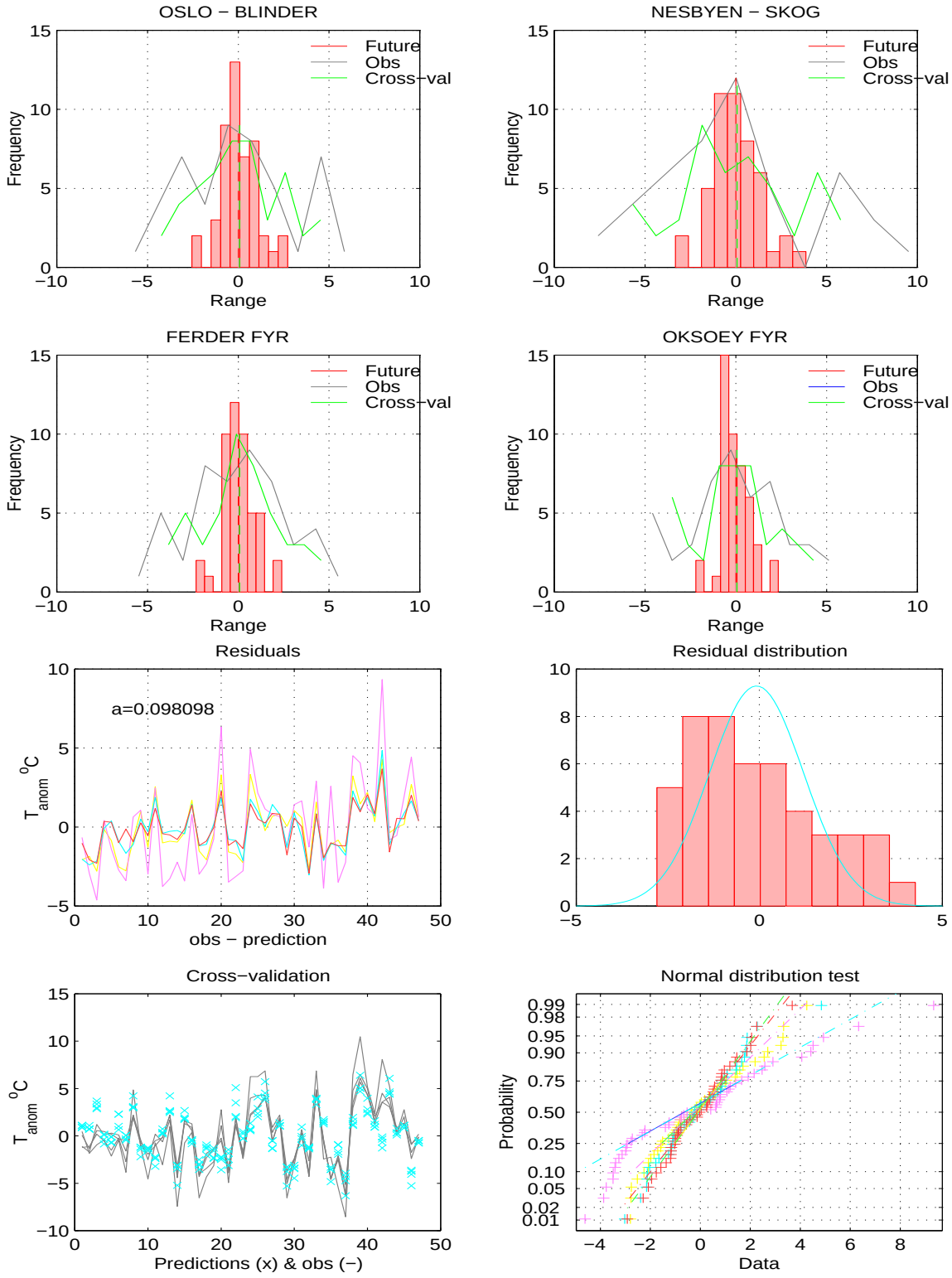

Figure 4: The temperature distributions (the four upper panels) and the residual statistics from the standard downscaling procedure (lower four panels).

Table 4: Observed past (1890-1997) and predicted January temperature trends using SLP common EOFs.

Location	Mean trend (^oC/decade)	Std (^oC/decade)	Uncertainty (%)
Mean trend	0.1663	0.0932	56
Mean CCA	0.1539	0.1187	77
Mean SVD	0.1743	0.0757	43
Mean MVR	0.1648	0.1002	61
Mean standard II	0.2067	0.0776	38
Mean NATL	0.1238	0.0835	67
Mean NORDIC	0.1361	0.1025	75
Mean SCAN	0.2232	0.0902	40
CCA-SVD T-test	CCA-MVR T-test	MVR-SVD T-test	
0.1443	0.0701	0.0752	
NATL-NORDIC T-test	NATL-SCAN T-test	SCAN-NORDIC- T-test	
0.0932	0.8088	0.6379	

residuals were absent for the experiment for which the historical SLP data had *not* been de-trended, may suggest that the recent (1950-1997) winter warming was related to long term changes in the circulation pattern. *Benestad* (1999a) argued that it is important to remove any trend prior to model calibration, and then apply the model to the original data (with long term trends) when studying the cause of low frequency climate changes. *Benestad* (1999a) concluded that the warming in Norway between 1880 and 1998 was not due to systematic changes in the NAO.

The lower left panel shows the results from the cross-validation analysis, and it is evident from this plot that the temperatures tend to follow changes in the large scale circulation. The January SLP fields may therefore be considered as a good predictor for January temperatures in southern Norway.

The right bottom panel and right second lower panel show the best Gaussian fit to the residuals. The poor fit can be explained by the linear trend in the residuals.

3.1 The effect of re-scaling the predictions

Figure 3a of the standard downscaling results, exhibits a dramatic drop in the predicted temperature variance, compared to the cross-validation. This systematic underestimation of the future temperature amplitudes is due to systematic errors in the GCM results, as the same empirical downscaling model almost reproduced the observed amplitudes in a cross-validation anal-

ysis. The predictions may therefore be re-scaled, which means multiplied by a scaling factor in order to increase the predicted standard deviation to the same value as that of the cross-validation results. The rescaling of the predictions, is shown in figure 3b.

The rescaling doesn't merely affect the amplitude of the signal, but also the trend estimates. Table 1 shows that the trend deduced for Oslo increased from 0.2506 for the standard procedure, to 0.6003 for the re-scaled predictions. This large difference of more than a factor of 2 is partly due to the short length of the prediction interval.

Any ad hoc re-scaling, such as described here, represent a potentially dangerous fudge factor, and should be done with care. As shown here, the re-scaling of the scenarios result in unrealistically high trends. Although, the amplitudes of the re-scaled temperatures were similar to those of those from the cross-validation analysis, we don't know if these are really true, as the re-scaling procedure only is a type of model output statistics (MOS) correction based on the assumption that the downscaled results ought to have similar standard deviation as the cross-validation. The drop in variance with the GCM predictors may suggest that there are some serious systematic errors in the dynamical model.

3.2 The effect of using time lengths

The entire length of the GSDIO model results (191 years) was combined with 51 years of observations, and a new set of common EOFs (comeof_ncep_slp-mpi-gsdio_slp_Jan_dl.nc) were computed for this combined field. The predictions based on this set of EOFs are shown in figure 3c. The future scenarios have even smaller amplitudes than those of the standard method, and table 1 show even smaller trends than the standard predictions. In fact, this experiment suggests similar trends for the future as seen in the past.

3.3 The effect of de-trending of the calibration period

The results from the downscaling experiment were the observations were not de-trended (comeof_ncep_slp-mpi-gsdio_slp_Jan_trend.nc) prior to the calculation of the common EOFs and calibration of the empirical model are shown in figure 3d. The comparison with the standard method suggests that the trends in the observed SLP fields did not affect the results very much. Table 1 suggests weaker future warming than the standard method suggests. Thus, in this case, the presence of linear trends in the observations reduced the estimated long term warming, rather than inflating the estimates (*Benestad*, 1999a).

3.4 The effect of using different predictand groups

Benestad (1999e) found that the downscaled future climate scenarios were sensitive to which stations were included in the predictand data set. The empirical models are optimised with respect to predictor patterns and this sensitivity was explained in terms of different circulation patterns influencing different locations and that the model was over-fit for the individual stations. *Benestad* (1999e) also speculated whether the matching between observed and simulated climate patterns was sensitive to the choice of predictands.

Table 1 shows standard scenarios for Oslo based on experiments using 3 different combinations of predictand stations. With station group *I* (Oslo, Ferder, Oksøy and Nesbyen), the estimated mean warming for Oslo in the period () is 0.2506°/decade. The correlation score for the cross-validation of the model was $r = 0.79$, whereas the root mean square error (RMSE) was 0.26°. Station group *II* (Oslo and Nesbyen) gave a slightly lower warming estimate of 0.2368°/decade, but the cross-validation analysis suggested slightly better skill ($r = 0.80$). The lowest cross-validation scores and temperature trends were obtained with station group *III* (Oslo, Ferder, and Oksøy). *Benestad* (1999e) observed that there was no direct relationship between the cross-validation scores and the trend estimate.

3.5 Standard method with SVD model

Table 4 lists the mean and spread in slopes of the temperature scenarios. The SVD models gave on average slightly higher long term trends (0.1743°/decade) as the CCA models (0.1539°/decade), but these were not statistically significant according to a simple students *t*-test. The cross-validation scores were also of similar magnitude as those of the CCA models. The spread between the CCA and the SVD estimates can be regarded as random errors, and can be used as a measure of uncertainty.

3.6 Standard method with MVR model

The mean of the downscaled scenarios from the MVR model (0.1648°/decade) suggested similar future warming trends as the CCA and the SVD, and was not statistically significant from either.

3.7 Sensitivity to predictor regions

Figure 5 shows the maps of the predictor area used in the different region studies. Four different regions were used for the predictor set: Standard

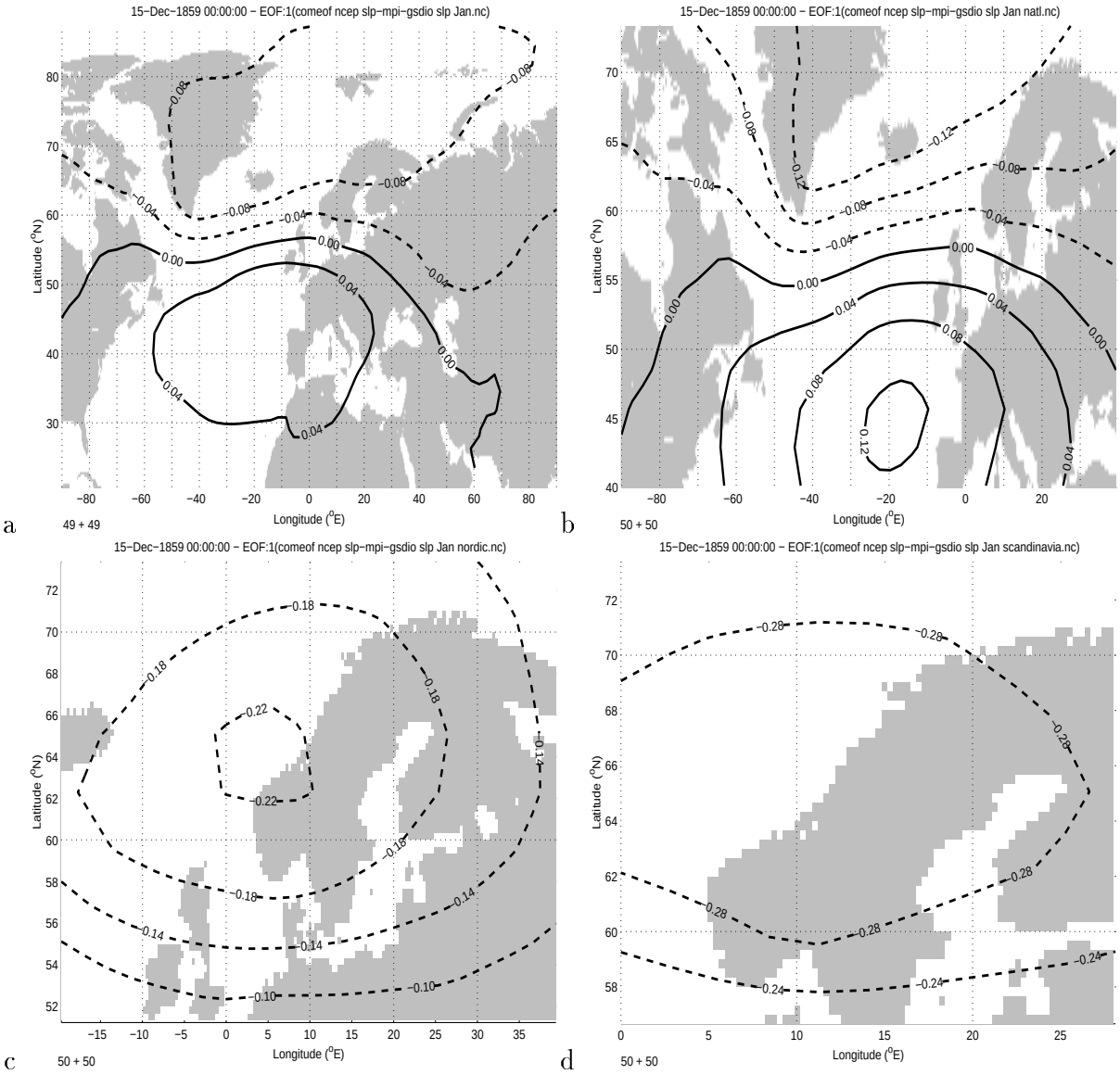

Figure 5: Standard procedure (a), the North Atlantic (b), Nordic (c), and Scandinavian (d) regions.

region (90°W-90°E, 20°N-90°N), NATL (90°W-40°E, 40°N-75°N), NORDIC (20°W-40°E, 50°N-75°N), and SCAN (0°W-30°E, 55°N-75°N). Table 2 and table:trend3 list the predicted trends (second column) cross-validation scores (third and fourth columns). A systematic decrease in the cross-validation scores from the standard region to smaller predictor are is evident for all model types. Table 4 shows the differences between the mean trends due to the various predictor domains. The NATL (0.1238°/decade) and NORDIC (0.1361°/decade) models give lower trends on average than the SCAN (0.2232) for experiments with station groups II and V. The corresponding mean trends for the standard model was 0.1663°/decade for all standard model experiments and 0.2067°/decade for experiments with station group II only. A students *t*-test reveals that these differences are not statistically significant.

4 Discussion and Conclusion

Trend uncertainties of future scenarios for Norway can be estimated in a crude fashion from the mean and standard deviation of the Oslo predictions. The mean trends and standard deviations are shown in table 4. The mean trend in the Oslo temperatures that could be explained in terms of systematic changes in the circulation pattern was 0.1576°C/decade according to table 4, with a standard deviation of 0.0818°C/decade. If we define the uncertainty as ±100*Std(trends)/mean(trends), then we get ±56% for the whole set of experiments with the standard model (excluding the re-scaling experiment). If we assume that the results for Oslo are typical for all stations, then the error bars of the trend estimates can be taken as $e \approx \pm 50\%$. For comparison, 15 of the entries for Nesbyen in column 2 of tables 1 to table:trend3 (excluding the re-scaled experiment) gave a mean trend of 0.2659°C/decade and a standard deviation of 0.1091. The estimated uncertainty for the predicted warming at Nesbyen is therefore 41%, and within the error bars estimated for Oslo. The uncertainty limits for Oksøy lighthouse was (14 scenarios: mean=0.1249, Std=0.0585) 47%.

Although the common EOF methodology was associated with some degree of uncertainty, it was believed that the source of most of the errors came from systematic GCM biases and the linear assumption that the temperatures were linearly related to the SLP fields, $\vec{y} = \Psi\vec{x}$. The main conclusion is therefore that the common EOF method is a good way of downscaling GCM results to local climate. The method leaves less choices, such as how to match observed patterns with he simulated ones, for subjective judgment than conventional methods. Furthermore, the common EOF frame work is also ideal for non-linear downscaling, $\vec{y} = \Psi(\vec{x})$, such as neural networks and

classification schemes. Together with estimating the long-term mean change by best the fit of linear trends for given long intervals (*Benestad*, 1999c), the common EOF method provides a sound framework for future empirical downscaling.

The scenarios shown here were solely based on the SLP fields (circulation pattern) from the GSDIO. The common EOF method and the ECHAM4/OPYC3 *GSDIO* results predict a future warming in Oslo of around 0.16 ± 0.08°C/decade. *Benestad* (1999c), in contrast, used a conventional linear downscaling method (pattern matching) and ECHAM4/OPYC3 *GHG* results and found no indication of any future warming related to the SLP patterns[2].

[2]The predictand data set used by *Benestad* (1999c) was from the NACD data set, whereas we have used temperatures from the DNMI archive here. The differences between the two data sets is minor (*Benestad*, 1999c).

References

Barnett, T.P. 1999. Comparison of Near-Surface Air Temperature Variability in 11 Coupled Global Climate Models. *Journal of Climate*, **12**, 511–518.

Benestad, R.E. 1996. *Conversion of the NCEP re-analysis data to the netCDF format and quality control.* KLIMA 31/99. DNMI, PO Box 43 Blindern, 0313 Oslo, Norway.

Benestad, R.E. 1998a. *CCA applied to Statistical Downscaling for Prediction of Monthly Mean Land Surface Temperatures: Model Documentation.* Klima 28/98. DNMI, PO Box 43 Blindern, 0313 Oslo, Norway.

Benestad, R.E. 1998b. *SVD applied to Statistical Downscaling for Prediction of Monthly Mean Land Surface Temperatures: Model Documentation.* Klima 30/98. DNMI, PO Box 43 Blindern, 0313 Oslo, Norway.

Benestad, R.E. 1999a. The cause of warming over Norway in the ECHAM4/OPYC3 *GHG* integration. *International Journal of Climatology*, Submitted.

Benestad, R.E. 1999b. *Conversion and quality control of the ECHAM4/OPYC3 GSDIO data to the netCDF format and a brief introduction to Ferret.* KLIMA 27/99. DNMI, PO Box 43 Blindern, 0313 Oslo, Norway.

Benestad, R.E. 1999c. *Evaluation of Seasonal Forecast Potential for Norwegian Land Temperatures and Precipitation using CCA.* Klima 23/99. DNMI, PO Box 43 Blindern, 0313 Oslo, Norway.

Benestad, R.E. 1999d. *MVR applied to Statistical Downscaling for Prediction of Monthly Mean Land Surface Temperatures: Model Documentation.* Klima 2/99. DNMI, PO Box 43 Blindern, 0313 Oslo, Norway.

Benestad, R.E. 1999e. *Pilot Studies of Enhanced Greenhouse Gas Scenarios for Norwegian Temperature and Precipitation from Empirical Downscaling.* Klima 16/99. DNMI, PO Box 43 Blindern, 0313 Oslo, Norway.

Benestad, R.E. 1999f. *S-mode and T-mode EOFs from a GCM modeller's perspective: Notes on the linear algebra.* Klima 24/99. DNMI, PO Box 43 Blindern, 0313 Oslo, Norway.

Benestad, R.E., Hanssen-Bauer, I., Førland, E.J., Tveito, O.E., & Iden, K. 1999. *Evaluation of monthly mean data fields from the ECHAM4/OPYC3*

control integration. Klima 14/99. DNMI, PO Box 43 Blindern, 0313 Oslo, Norway.

Machenhauer, B., Windelband, M., Botzet, M., Christensen, J.H., Déqué, M., Jones, R.G., Ruti, P.M., & Visconti, G. 1998. *Validation and Analysis of Regional Present-day Climate and Climate Change Simulations over Europe*. Tech. rept. 275. Max Planck-Institute für Meteorologie.

Rew, R., Davis, G., Emmerson, S., & Davies, H. 1996. *NetCDF User's Guide*. Unidata Program Center.

5 Appendix